Cytotechnology (2017) 69:711–724
DOI 10.1007/s10616-017-0079-2

Differential effects of p38 MAP kinase inhibitors SB203580 and SB202190 on growth and migration of human MDA-MB-231 cancer cell line

Şükrü Aydın Düzgün · Azmi Yerlikaya · Sezgin Zeren · Zülfü Bayhan · Emrah Okur · İhsan Boyacı

Received: 24 August 2016 / Accepted: 9 March 2017 / Published online: 9 April 2017

Abstract p38 mitogen-activated protein kinase (MAPK) belongs to the MAPK superfamily, phosphorylating serine and/or threonine residues of the target proteins. The activation of p38 MAPK leads to cell growth, differentiation, inflammation, survival or apoptosis. In this study, we tested the effect of two highly specific and potent inhibitors of p38 MAPK (namely, SB203580 and SB202190) on human breast cancer cell line MDA-MB-231 to elucidate the controversial role of p38 MAPK on cell proliferation and/or cell migration/metastasis further. It was determined that the IC_{50} value of SB203580 was 85.1 μM, while that of SB202190 was 46.6 μM, suggesting that SB202190 is slightly more effective than SB203580. To verify the effect of each inhibitor on cell proliferation and cytotoxicity, the cells were treated with various doses of SB203580 and SB202190 and examined using iCELLigence system. No significant effect of 1 and 5 μM of both inhibitors were seen on cell proliferation as compared to the DMSO-treated control cells for up to 96 h. On the other hand, both SB203580 and SB202190 significantly prevented cell proliferation at a concentration of 50 μM. SB202190 was again more effective than SB203580. Afterwards, we tested the effect of each inhibitor on cell migration using wound assay. Both SB203580 and SB202190 significantly reduced cell migration in a time-dependent manner at a concentration of 50 μM. However, interestingly it was observed that a low and noncytotoxic dose of 5 μM of SB203580 and SB202190 also did cause significant cell migration inhibition at 48 h of the treatment, corroborating the fact that p38 MAPK pathway has a critical role in cell migration/metastasis. Then, we tested whether each p38 MAPK inhibitor has any effect on cell adhesion during a treatment period of 3 h using iCELLigence system. A concentration of only 50 μM of SB202190 reduced cell adhesion for about 1.5 h ($p < 0.001$); after that period of time, cell adhesion in 50 μM SB202190-treated cells returned to the level of the control cells. To determine the mechanism of growth and cell migration inhibitory effects of p38 MAPK inhibitors, the activation/inactivation of various proteins and enzymes was subsequently analyzed by PathScan®

Ş. A. Düzgün
Department of General Surgery, Jimer Hospital, Bursa, Turkey

A. Yerlikaya (✉)
Department of Medical Biology, Faculty of Medicine, Dumlupınar University, Kutahya, Turkey
e-mail: azmi.yerlikaya@dpu.edu.tr

S. Zeren · Z. Bayhan
Department of General Surgery, Faculty of Medicine, Dumlupınar University, Kutahya, Turkey

E. Okur
Department of Biology, Art and Science Faculty, Dumlupınar University, Kutahya, Turkey

İ. Boyacı
Vatan Clinic, Medical School, İstanbul Medipol University, Istanbul, Turkey

Intracellular Signaling Array kit. The ERK1/2 phosphorylation level was not modified by low concentrations (1 or 5 μM) of SB202190 and SB203580; while a high concentration (50 μM) of both inhibitors caused significant reductions in the ERK1/2 phosphorylation. In addition, it was determined that both p38 MAPK inhibitors caused significant increases on the Ser15 phosphorylation of mutant p53 in MDA-MB-231 under these experimental conditions; while SB202190 was more potent than SB203580.

Keywords Cancer · p38 MAPK · Proliferation · Metastasis

Introduction

p38 mitogen-activated protein kinase (MAPK) is a subgroup of MAPK pathways which phosphorylate serine and/or threonine residues of the target proteins, subsequently regulating a number of biological processes, including cell growth, differentiation, apoptosis and inflammation (Koul et al. 2013). Four different isoforms of p38 MAPKs have been identified: p38α, β, γ and δ, which also are known as stress-activated protein kinase 2a (SAPK2a), SAPK2b, SAPK3 and SAPK4, respectively (Porras and Guerrero 2011). The p38 MAPK pathway is activated in response to various signals such as osmotic shock, oxidative stress, iron depletion and cytokines (Porras and Guerrero 2011; Lawson et al. 2013). Kumar et al. (2009) demonstrated that ERK1/2 and p38 MAP kinase are active during the logarithmic growth phase of bladder cancer; and inhibition of these two pathways by PD98059 (Erk1/2 inhibitor) or SB203580 (p38 inhibitor) for 72 h in HTB5 and HTB9 bladder carcinoma cells could reduce the proliferation and growth. Similarly, it was shown that photodynamic therapy causes induction of HO-1 expression, an antioxidant and cytoprotective protein, through the activation of p38 MAPK and PI3K signaling cascades (Kocanova et al. 2007). On the other hand, p38 MAPKs can also regulate cell death through different mechanisms depending on cell type, the stimuli and/or isoforms (Porras and Guerrero 2011). The induction of apoptosis by TNF-α in rat fetal brown adipocytes (Valladares et al. 2000) or by TGF-β in prostate cancer cells (Edlund et al. 2003) or by oxidative stress (Zhuang et al. 2000) involves p38α and/or p38β MAPKs as mediators of apoptosis. Consistent with these observations, a number of evidence indicated that p38α plays a key role in the regulation of the tumor suppressor protein p53, a critical mediator of apoptotic cell death in response to a great variety of stimuli (Porras and Guerrero 2011). However, in contrast to these results, Gutiérrez-Uzquiza et al. (2012) indicated that p38 mediates cell survival in response to oxidative stress (0.1–1 mM H_2O_2) via induction of antioxidant genes (SOD-1, SOD-2 and catalase).

The activation of p38 MAPK is also critical for cell migration, invasion and metastasis (Koul et al. 2013; Huang et al. 2000; del Barco Barrantes and Nebreda 2012). For example, Huang et al. (2000) showed that T47D and MDA435 breast cancer lines, which exhibited low levels of p38 MAPK activity, were unable to invade matrigel; whereas, BT549, MDA231 and MDA436 breast cancer cells, having high endogenous p38 MAPK activity, showed significant matrigel invasion, suggesting a correlation between constitutive p38 MAPK activity and the invasiveness of human breast cancer cells. The authors also showed treatment of highly invasive BT549 cells with a specific p38 MAPK inhibitor SB203580 diminished both uPA/uPAR mRNA and protein expression and abrogated the ability of these cells to invade matrigel, suggesting that p38 MAPK signaling pathway is involved in the regulation of uPA/uPAR expression as well as breast cancer cell invasion (Huang et al. 2000).

To elucidate the controversial role of p38 MAPK on cell proliferation and/or cell migration/metastasis further, we tested the effect of two highly specific and potent inhibitors of p38 MAPK SB203580 4-(4-fluorophenyl)-2-(4-methylsulfinylphenyl)-5-(4-pyridyl)-imidazole) and SB202190 4-(4-fluorophenyl)-2-(4-hydroxyphenyl)-5-(4-pyridyl)-imidazole on human breast cancer cell line MDA-MB-231. It was found that both inhibitors were cytotoxic at higher concentrations using MTT assay in MDA-MB-231 breast cancer cell line. The real-time iCELLigence system unexpectedly showed that low doses of both inhibitors had growth-promoting effects; however, the cell proliferation was only inhibited by quite high concentrations of both inhibitors (i.e., 50 μM). Using the PathScan Intracellular Signaling Array Kit, significant changes in the phosphorylation of ERK1/2, S6 ribosomal protein, mutant p53, PRAS40 and p38 enzymes

were detected in response to p38 MAPK inhibitors used in the current study.

Materials and methods

Materials

RPMI-1640 cell culture medium, trypsin, penicillin/streptomycin, fetal bovine serum (FBS), MTT [3-(4.5-dimethylthiazol-2-yl)-2.5-diphenyl-tetrazolium bromide] and Kodak BioMax X-ray films were obtained from Sigma Aldrich Inc. (Steinheim, Germany). P38 inhibitors SB203580 and SB202190 and PathScan Intracellular Signaling Array Kit (Chemiluminescent Readout) were obtained from Cell Signaling Technology Inc. (Danvers, MA, USA). E-Plate L8 was from ACEA Biosciences (San Diego, CA, USA). All other reagents were purchased from Sigma Aldrich Inc. (Steinheim, Germany) unless otherwise mentioned.

Cell culture maintenance

MDA-MB-231 human breast cancer cell line was cultured in RPMI-1640 containing 4.5 g/L glucose, 10 mM HEPES, 1 mM sodium pyruvate, 0.15% sodium bicarbonate, 100 µg/ml streptomycin and 100 U/ml penicillin. The medium was supplemented with 10% fetal bovine serum (FBS). The cell line was grown in 25 cm^2 corning flasks (Corning Incorporated, Corning, NY, USA) for passages. For the experiments, the cells were grown in 35 × 10 mm Corning dishes, 60 × 15 mm Corning dishes or E-Plate L8. The cells were subcultured upon reaching about 70% confluence (Yerlikaya and Dokudur 2010; Yerlikaya et al. 2012).

MTT-based cytotoxicity assay

MDA-MB-231 cells (100,000) were seeded in each 35 × 10 mm dish. Cells were treated at the logarithmic phase of the growth (Yerlikaya and Erin 2008) with various doses of SB203580 (0.1, 0.5, 1, 5, 10, 25, 50, 100 µM) or SB202190 (0.1, 0.5, 1, 5, 10, 25, 50, 100 µM) for 24 h. Following the inhibitor exposure period, the medium was changed with RPMI-1640 containing 0.5% FBS + 0.5 mg/ml MTT, the cells were incubated for another 4 h at 37 °C with 5% CO_2. After MTT treatment, cells were lysed with 200 µl 3% SDS plus 1 ml 40 mM HCl/isopropanol for 15 min. After dissolving the MTT-formazan crystals, the cell lysate was diluted with 3% SDS + 40 mM HCl/isopropanol. Finally, each sample absorbance was recorded at 570 nm with a SmartSpec Plus spectrophotometer (Bio-Rad Laboratories, Inc., Hercules, CA, USA). The data were analyzed and graphed with GraphPad Prism 5 program (GraphPad Software, Inc., La Jolla, CA, USA) (Freshney 2005; Yerlikaya and Erin 2008). The IC_{50} values were then obtained by GraphPad Prism 5 program using nonlinear regression to fit the data to the log(inhibitor) versus normalized response.

Wound assay

MDA-MB-231 human breast cancer cells were grown in 35 × 10 mm sterile petri dishes. The cells were cultured to at least 90% confluence. Using a 200 µl sterile pipet tip, three separate wounds were scratched in each petri dish. Afterwards, the cells were treated with 0.5% DMSO (control), 5 µM SB203580, 50 µM SB203580, 5 µM SB202190 or 50 µM SB202190 for 24 h. Mitomycin C (10 µg/ml) was added to all experimental plates to block cell proliferation (Li et al. 2004). The migration and morphology of cells were recorded with an inverted microscope using a 4× objective (AE21; Motic Europe, Barcelona, Spain) (Liang et al. 2007; Koçak et al. 2013).

iCELLigence system

The effects of SB203580 and SB202190 inhibitors on proliferation and adhesion of MDA-MB-231 cells were determined by using the iCELLigence system. Cells were seeded in E-plate L8 that have integrated microelectrode sensors in the bottom of the wells. As the cells proliferate and adhere to the micro-electrodes, changes in electrical impedance occur that reflects the biological status of the cells, thus the system allows monitoring of time-dependent effects on a cell culture. The information about the cell status is expressed in terms of cell index (CI). For cell proliferation, 12,500 cells were seeded in each well of E-plate L8, and the inhibitors (10 nM SB203580, 100 nM SB203580, 500 nM SB203580, 1 µM SB203580, 5 µM SB203580, 50 µM SB203580, 10 nM SB202190, 100 nM SB202190, 500 nM SB202190, 1 µM SB202190, 5 µM SB202190 or

50 μM SB202190) were added to the wells after 24 h of seeding in the logarithmic phase of the growth. The cells were then incubated at 37 °C, 5% CO_2 for 96 h. The cell index (CI) was monitored every hour by the iCELLigence system (Aras and Yerlikaya 2016). Cell adhesion was determined for a period of 3 h. 20,000 cells were seeded in each well in E-plate L8. Then the inhibitors (1 μM SB203580, 5 μM SB203580, 50 μM SB203580, 1 μM SB202190, 5 μM SB202190 or 50 μM SB202190) were added immediately after cell seeding. The cells were incubated at 37 °C, 5% CO_2 for about 3 h. Cell adhesion was observed by iCELLigence system.

Analysis of intracellular signaling molecules

Phosphorylation or cleavage of 18 well-characterized signaling molecules [ERK1/2 (Thr202/Tyr204), Stat1 (Tyr701), Stat3 (Tyr705), Akt (Thr308), Akt (Ser473), AMPKa (Thr172), S6 Ribosomal Protein (Ser235/236), mTOR (Ser2448), HSP27 (Ser78), Bad (Ser112), p70 S6 Kinase (Thr389), PRAS40 (Thr246), p53 (Ser15), p38 (Thr180/Tyr182), SAPK/JNK (Thr183/Tyr185), PARP (Asp214), Caspase-3 (Asp175), GSK-3b (Ser9)] were detected using the PathScan Intracellular Signaling Array Kit (Chemiluminescent Readout), according to the manufacturer's procedure (Cell Signaling Technology). MDA-MB-231 human breast cancer cells (200,000) were seeded in 60 × 15 mm sterile petri dishes. Cells were treated with 1 μM SB203580, 5 μM SB203580, 50 μM SB203580, 1 μM SB202190, 5 μM SB202190 or 50 μM SB202190 at the logarithmic phase of the growth for 24 h. After inhibitor treatments, the medium was removed. Cells were washed with ice-cold 1× PBS and then 0.3 ml of ice-cold cell lysis buffer was added to each plate and incubated on ice for 5 min. The lysate was centrifuged at 10,000×*g* at 4 °C for 10 min. After that, protein quantity was measured using the Bio-Rad dye-binding assay (bovine serum albumin as a standard). The glass slide array containing the antibodies for the proteins to be analyzed was affixed to the multi-well gasket. Afterwards, 100 μl array blocking buffer was pipetted to each well. The wells were covered with sealing tape and were incubated for 15 min at room temperature on an orbital shaker. After the blocking step, 75 μl of diluted lysate (45 μg protein) was pipetted to each appropriate well followed by an incubation for 2 h at room temperature on an orbital shaker. After washing the wells, 75 μl of 1× detection antibody cocktail was added to each well for another incubation for 1 h. Then, 75 μl of 1× HRP-linked streptavidin was pipetted to each well for 30 min at room temperature (Miyake et al. 2013). After washing steps, the slides were incubated with Lumi-GLO/peroxide reagent for 2 min and finally were exposed to Kodak BioMax X-ray films in dark room for an appropriate exposure time.

Statistical analysis

Results were analyzed and graphed using GraphPad Prism 5 software. The statistical differences between the inhibitor treatments were evaluated by one-way ANOVA and Bonferroni or Newman–Keuls Multiple Comparison Test. A p value <0.05 was considered significant.

Results

To investigate the controversial role of p38 MAP kinase on cell proliferation and cell migration/metastasis, we used two highly specific and potent inhibitors of p38 MAPK (i.e., SB203580 and SB202190). SB202190 inhibits p38 MAP kinase activity through competition with ATP and also inhibits p38 MAPK phosphorylation in spite of exposure to anisomycin, known to be an activator of the MAPK pathway (Geiger et al. 2005). On the other hand, SB203580 inhibits p38 MAPK catalytic activity by binding to the ATP-binding pocket but does not inhibit phosphorylation of p38 MAPK by upstream kinases (Kumar et al. 1999). Both SB202190 and SB203580 are known to be specific inhibitors of p38α and p38β isoforms (Nemoto et al. 1998; Sicard et al. 2010). First, we determined the cytotoxic effects of both inhibitors on human breast cancer cell line MDA-MB-231 by MTT assay. As can be seen in Fig. 1, both inhibitors did not cause significant cytotoxicity on human MDA-MB-231 breast cancer cell line at low concentrations (0.1–10 μM) as compared to vehicle-treated (0.5% DMSO) control cells ($p > 0.05$). However, the cytotoxic effects of both inhibitors were observed with higher concentrations of 25, 50 and 100 μM. It was determined that the IC_{50} value of SB203580 was 85.1 μM, while that of SB202190 was 46.6 μM, suggesting that SB202190 is slightly more

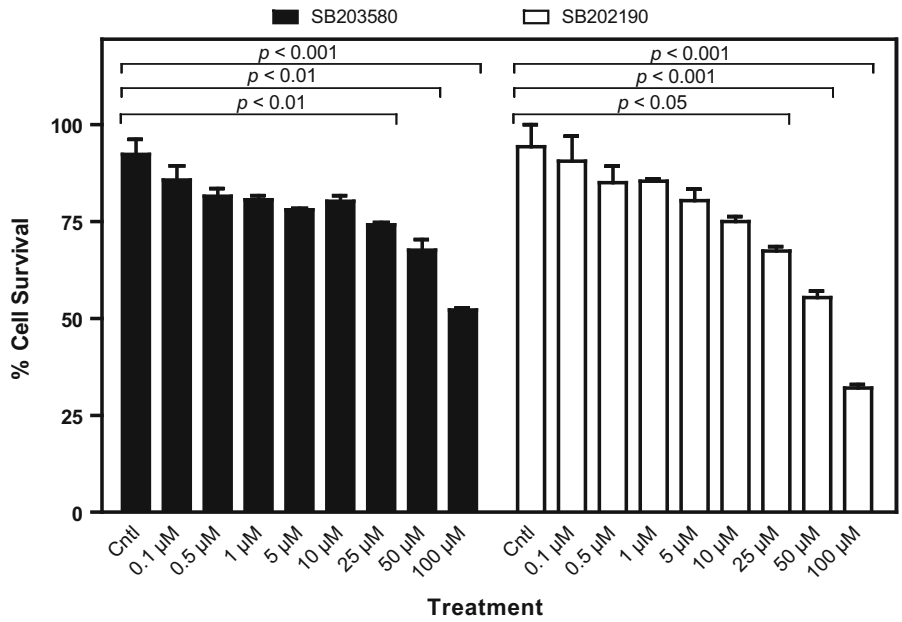

Fig. 1 Effect of p38 MAP kinase inhibitor SB203580 and SB202190 on human MDA-MB-231 cell line. Effects of SB203580 and SB202190 on the survival of MDA-MB-231 cells were determined by MTT assay. MDA-MB-231 cells (100,000) were plated on sterile 35 × 10 mm petri dishes and treated at the logarithmic phase of the growth with SB203580 (0.1, 0.5, 1, 5, 10, 25, 50 and 100 µM) or SB202190 (0.1, 0.5, 1, 5, 10, 25, 50 and 100 µM) for 24 h. Then, the number of surviving cells was determined by MTT assay. The results are presented as mean ± SEM (n = 3). Cntl, 0.5% DMSO-treated control group

effective than SB203580. To verify the effect of each inhibitor on cell proliferation and cytotoxicity, the cells were treated with various doses of SB203580 and SB202190 (1, 5 and 50 µM) and examined using iCELLigence system, an impedance-based system used for label-free and real-time monitoring of cytotoxicity, cell proliferation and cell adhesion. As seen in Fig. 2a, b, no significant effect of 1 and 5 µM of both inhibitors was seen on cell proliferation as compared to the DMSO-treated control cells for up to 96 h. On the other hand, both SB203580 and SB202190 significantly prevented cell proliferation at a concentration of 50 µM (Fig. 2a, b). SB202190 was again more effective than SB203580 (Fig. 2a, b). Interestingly, low doses of each inhibitor caused slight growth-promoting effects; in fact, treatment of MDA-MB-231 cells with low doses of both inhibitors (i.e., 10, 100 and 500 nM) indicated that 100 and 500 nM concentrations of SB203580 ($p < 0.01$ with both 100 and 500 nM concentrations) and SB202190 ($p < 0.05$ with 100 nM concentration; $p < 0.01$ with 500 nM concentration) enhanced cell proliferation (Fig. 2c, d). Furthermore, we tested the effect of each inhibitor on cell migration using wound assay in the presence of mitomycin C (10 µg/ml), added to all experimental plates to block cell proliferation (Li et al. 2004). Both SB203580 and SB202190 significantly reduced cell migration in a time-dependent manner at a concentration of 50 µM (Fig. 3a, b), causing significant cell migration inhibition starting at 12 h of incubation until 48 h of treatment ($p < 0.001$ at all time points for both inhibitors) (Fig. 3b). However, interestingly it was observed that a low and noncytotoxic dose of 5 µM of SB203580 and of SB202190 (Fig. 3a, b) also did cause significant cell migration inhibition at 48 h ($p < 0.01$ for both inhibitors), corroborating the fact that p38 MAPK pathway has a critical role in cell migration/metastasis. It is also concluded that since the experiment was carried out in the presence of mitomycin C (10 µg/ml), any scratch closure is not due to the cell proliferation. Then, we tested whether each p38 MAPK inhibitor has any effect on cell adhesion during a treatment period of 3 h using iCELLigence system. The inhibitors were added immediately after cell seeding (20,000 cells/E-plate L8 well). As seen in Fig. 4a, b, only 50 µM concentration of SB202190 reduced cell adhesion for about 1.5 h

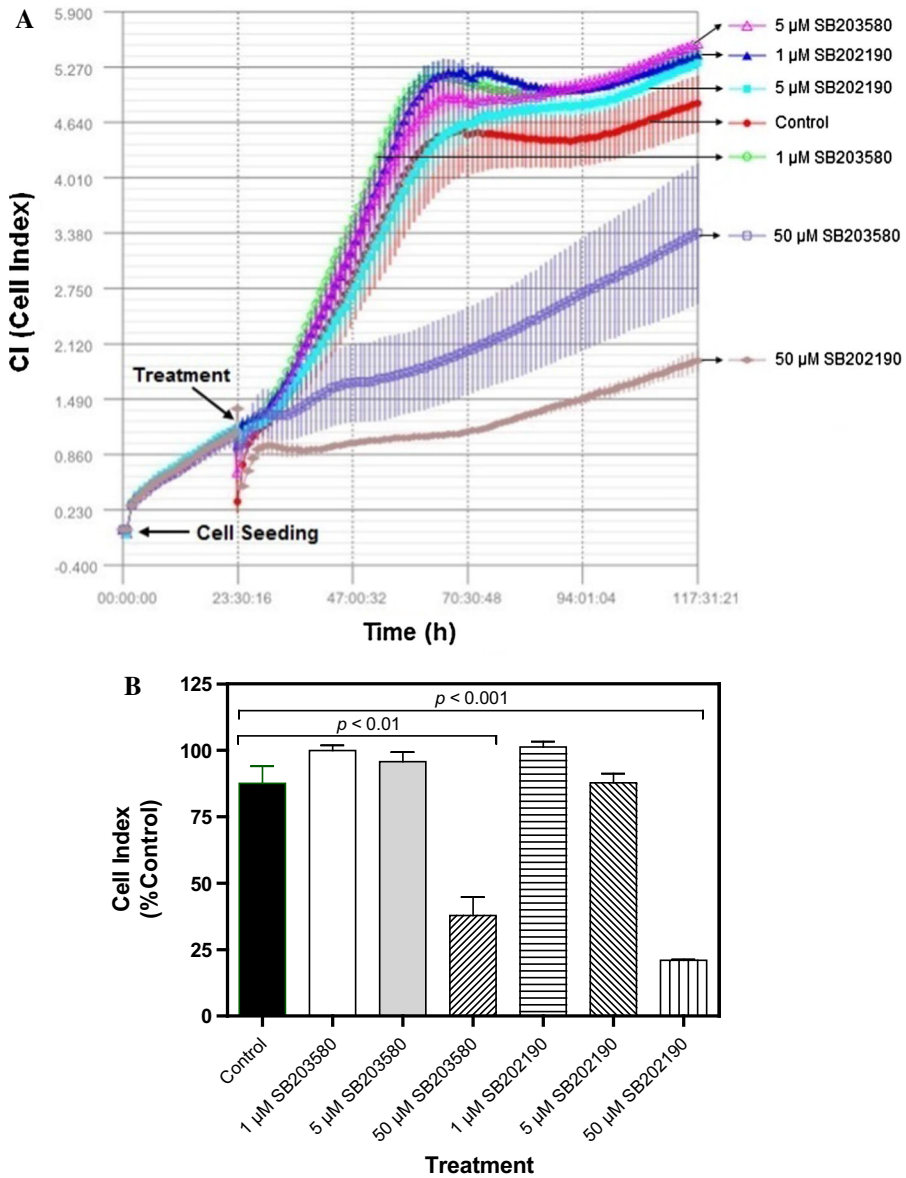

Fig. 2 Determination of effects of SB203580 and SB202190 on cell proliferation. **a** MDA-MB231 cells (12,500) were seeded in each well of E-plate L8 and treated with 1 μM SB203580, 5 μM SB203580, 50 μM SB203580, 1 μM SB202190, 5 μM SB202190 or 50 μM SB202190 for approximately 96 h. The cell index (CI) was monitored every hour by using the iCELLigence system. The results are mean ± standard deviation (n = 2 or 3), **b** proliferation values of MDA-MB-231 cells at the 42 h of inhibitor treatments. The results are presented as the mean ± SEM (n = 2 or 3), **c** effect of 10 nM, 100 nM and 500 nM of SB203580 and SB202190 on MDA-MB-231 cell proliferation, **d** graphical representation of the effect of low doses of SB203580 and SB202190 at the 42 h of inhibitor treatments. The results are presented as the mean ± SEM (n = 2 or 4). The *error bars* are not visible in some bars on account of small variations

($p < 0.001$); after that period of time, cell adhesion in 50 μM SB202190-treated cells returned to the level of the control cells. However, 1 μM SB202190, 5 μM SB202190, 5 μM SB203580 and 50 μM SB203580 did not change cell adhesion as compared to the control. Interestingly, similarly to the growth-promoting effects of low doses of both inhibitors (i.e., 100 and 500 nM of SB203580 and SB202190), 1 μM SB203580 increased cell adhesion contrary to our expectation ($p < 0.05$) (Fig. 4a, b). To determine the mechanism of growth and

Fig. 2 continued

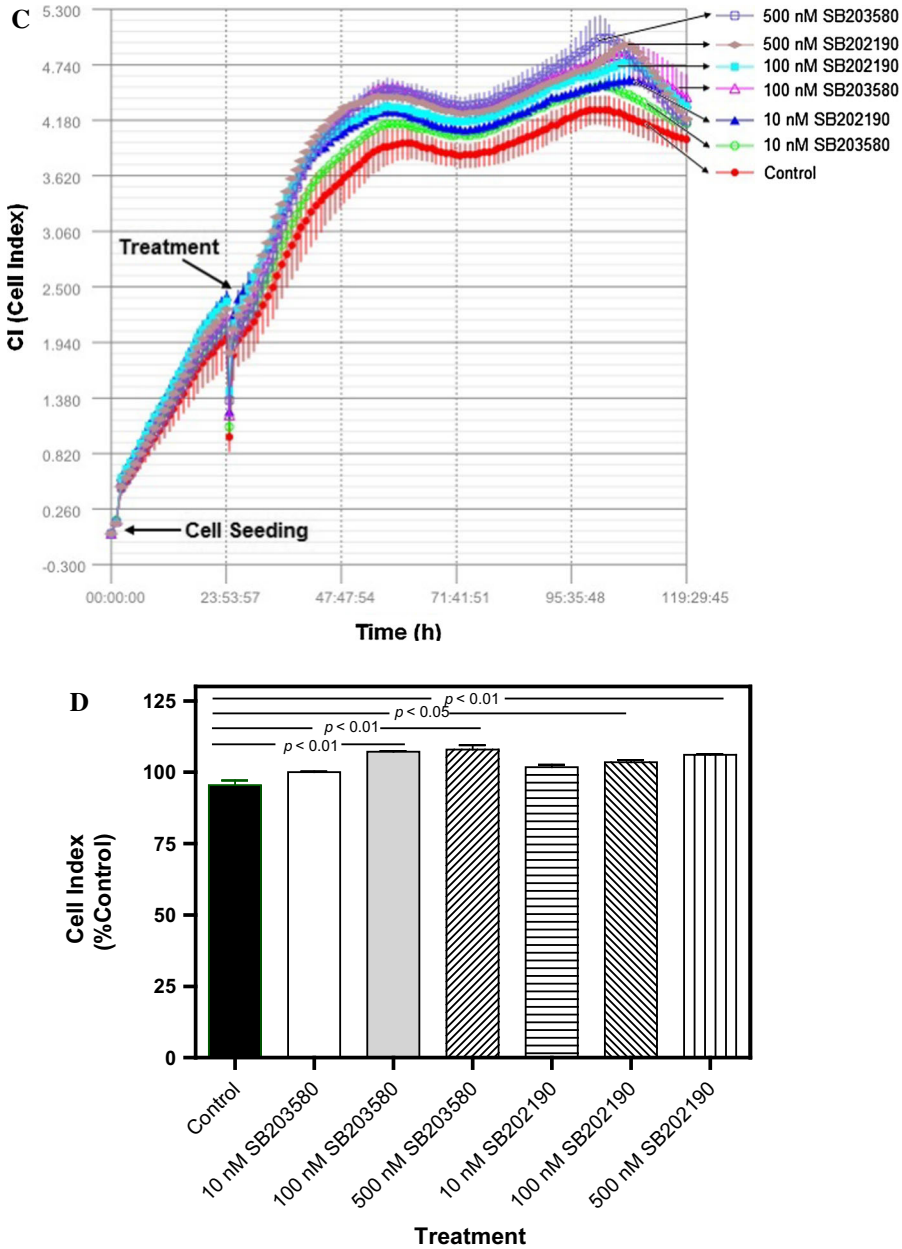

cell migration inhibitory effects of p38 MAPK inhibitors (1, 5 and 50 μM concentrations of SB203580 and SB202190 were used for 24 h), the activation/inactivation of various proteins and enzymes were subsequently analyzed by PathScan® Intracellular Signaling Array kit, a slide-based antibody array detecting phosphorylation or cleavage of 18 important signaling molecules. As shown by Fig. 5, we have detected changes in the phosphorylation level of five enzymes/proteins [i.e., ERK1/2 (Thr202/Tyr204 phosphorylated), S6 ribosomal protein (Ser235/236 phosphorylated), mutant p53 (Ser15 phosphorylated), PRAS40 (Thr246 phosphorylated) and p38 (Thr180/Tyr182)]. No significant changes in the phosphorylation or cleavage of 13 other enzymes/proteins stated in the "Materials and methods" section were detected under these experimental conditions (Fig. 5a). As seen in Fig. 5a, b, the phosphorylation level of ERK1/2, S6 ribosomal protein and PRAS40

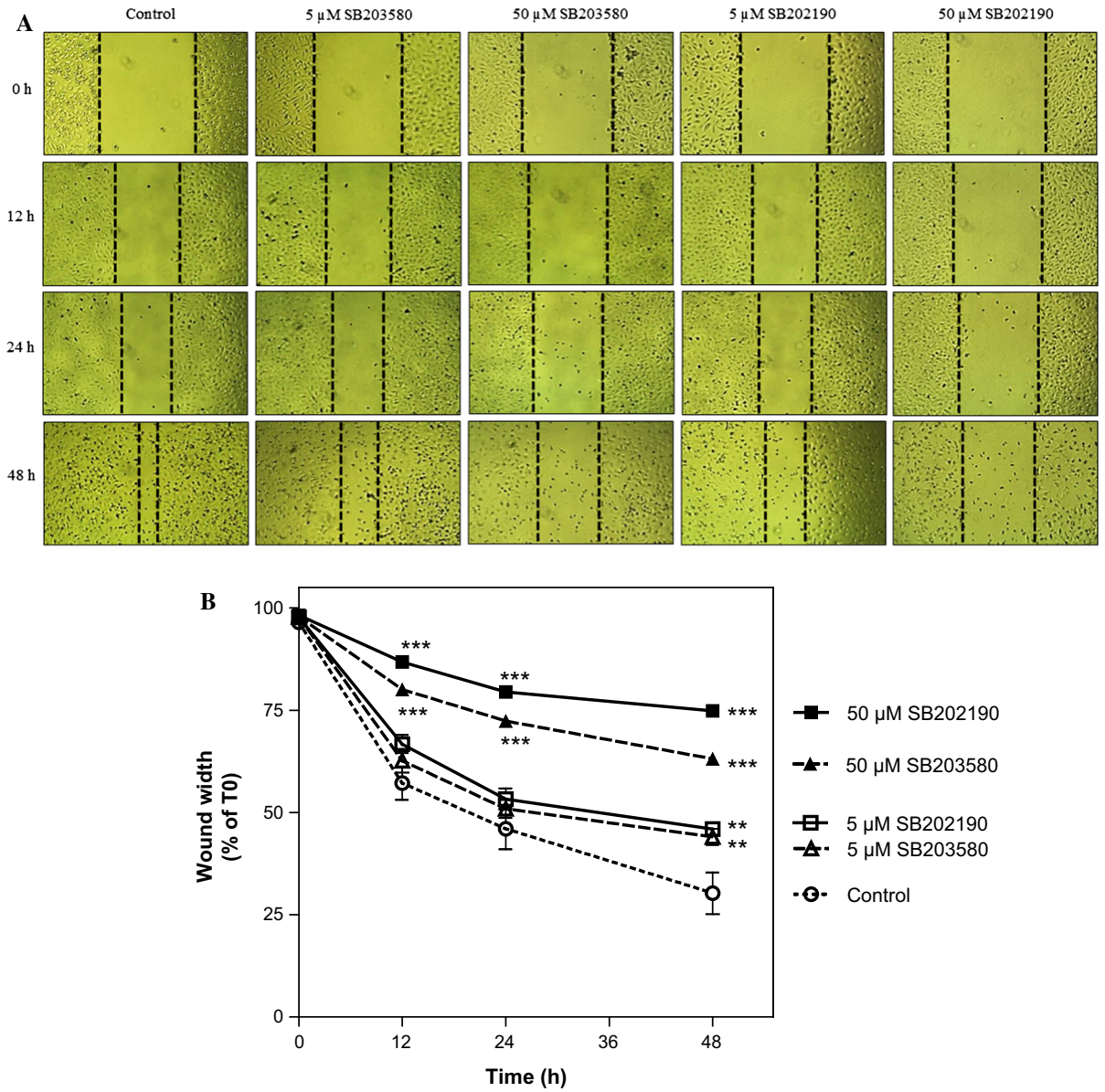

Fig. 3 Effect of SB203580 and SB202190 inhibitors on cell migration. **a** MDA-MB-231 cells were treated with various concentrations of SB203580 or SB202190 for 48 h. Cell migration and cell morphology were recorded with an inverted microscope. Mitomycin C (10 µg/ml) was added to all experimental plates to block cell proliferation, **b** graphical representation of cell migration. Quantitation of the cell migration by measuring the relative distance in each wound. The results are mean ± SEM (n = 6). $^{**}p < 0.01$; $^{***}p < 0.001$

were not changed by low concentrations of both inhibitors; however, while both inhibitors at a high concentration (50 µM) caused significant reductions in the phosphorylation of ERK1/2; phosphorylation of S6 ribosomal protein and PRAS40 was decreased significantly only by 50 µM concentration of SB202190. As can be seen in Fig. 5a, b, both inhibitors (SB202190 and SB203580) caused significant increases in the Ser15 phosphorylation of mutant p53 after treatment with 50 µM concentration of each inhibitor; however, SB202190 was more potent than SB203580. Interestingly, both SB203580 (at a concentration of 50 µM) and SB202190 (at concentrations of 1, 5 and 50 µM) treatments were associated with significant increases

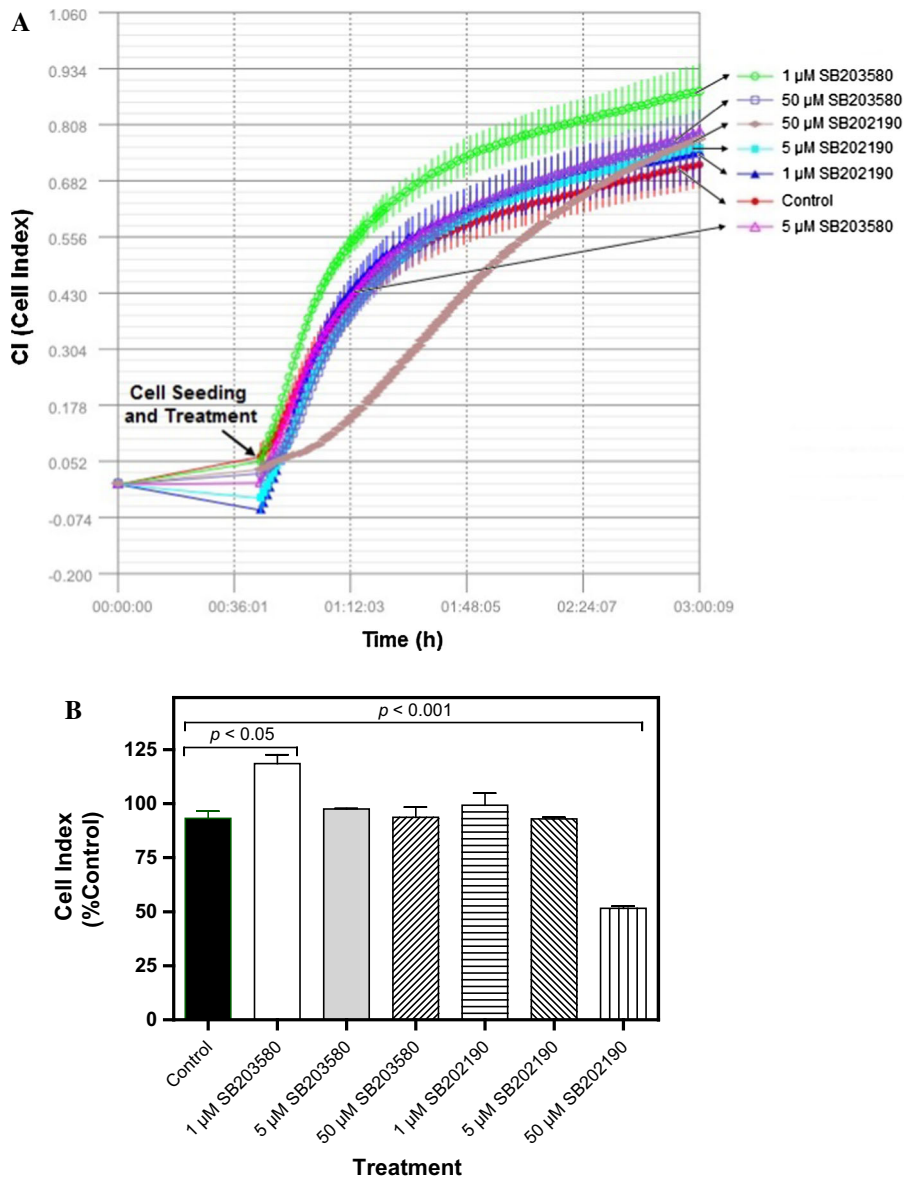

Fig. 4 Effects of SB203580 and SB202190 inhibitors on cell adhesion. **a** A total of 20.000 MDA-MB-231 cells/well were seeded in E-plate L8. Inhibitors (1 µM SB203580, 5 µM SB203580, 50 µM SB203580, 1 µM SB202190, 5 µM SB202190 or 50 µM SB202190) were pipetted immediately after cell seeding. Cell adhesion was observed for a period of 3 h using iCELLigence system. The results are expressed as the mean ± standard deviation (n = 2 or 4), **b** adhesion values of MDA-MB-231 cells at 46 min of treatments. The results are mean ± SEM (n = 2 or 4)

in p38 MAPK phosphorylation (at Thr180/Tyr182) (Fig. 5a, b). Although it is known that SB203580 inhibits the kinase activity of p38 MAP kinase, but does not prevent it from being phosphorylated (Xu et al. 2006), to our best knowledge, the increase in the phosphorylation of p38 MAPK in the presence of its inhibitor SB202190 was not reported before in MDA-MB-231 breast cancer cells. In consistence with our observations here, inhibition of p38 MAPK in HUVEC endothelial cell by 10 or 20 µM SB202190 for 40 min before treatment with TNF-α or lipopolysaccharide (LPS) caused an increase in the phosphorylation of p38 MAPK, while it inhibited both TNF-α and LPS induction of CREB and ATF-1 phosphorylation but not degradation of I-KBα (Stone et al. 2008).

Discussion

In the present study, we investigated the differential roles of p38 MAPK inhibitors SB203580 and SB202190 on cell growth, adhesion and migration on MDA-MB-231 breast cancer cell line. It was suggested that the tumor cells need to modulate p38

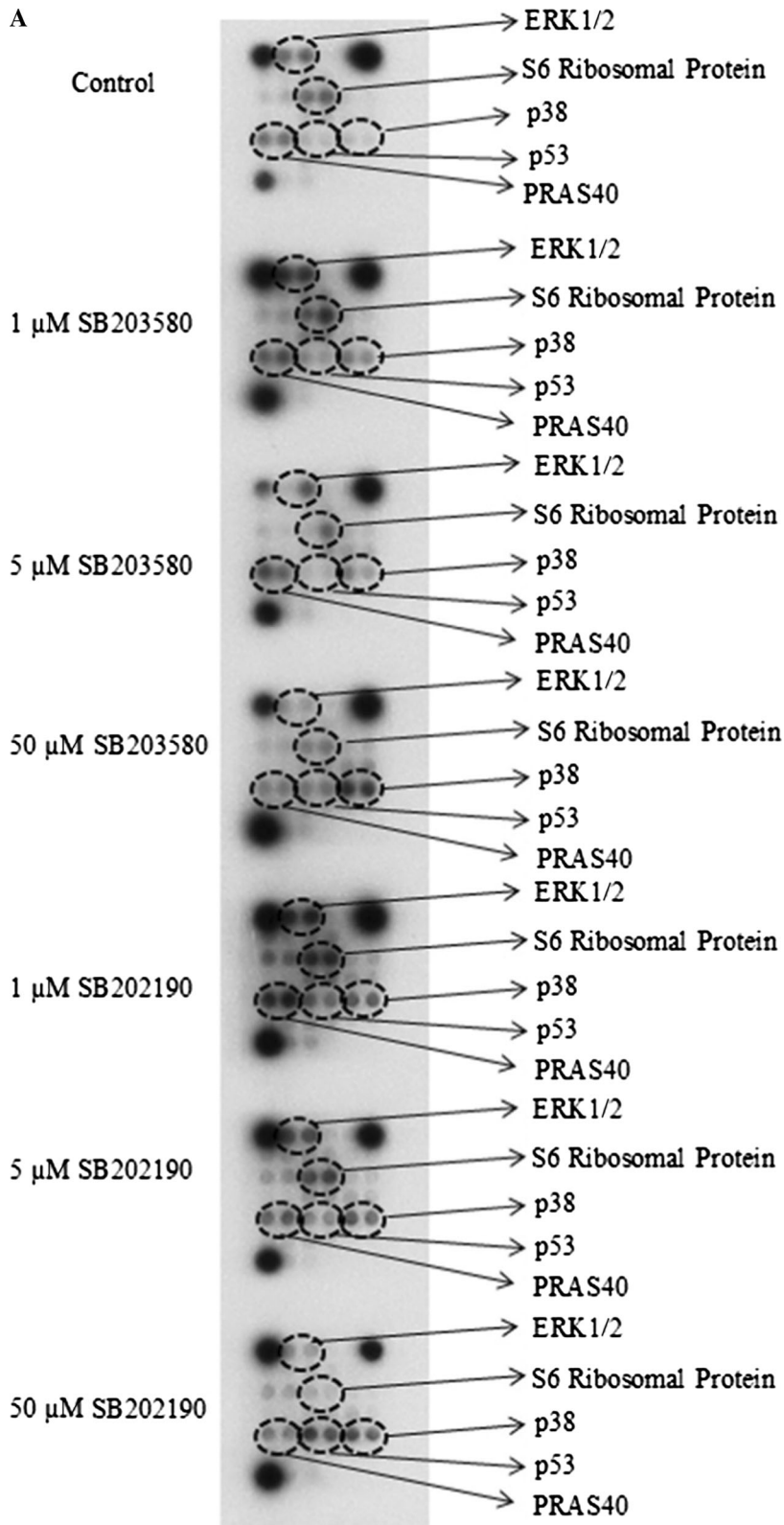

Fig. 5 Effects of SB203580 and SB202190 inhibitors on intracellular signaling molecules. **a** MDA-MB-231 human breast cancer cells (200,000) were seeded in 60 × 15 mm sterile petri dishes. Cells were treated with 1 μM SB203580, 5 μM SB203580, 50 μM SB203580, 1 μM SB202190, 5 μM SB202190 or 50 μM SB202190 at the logarithmic phase of growth for 24 h. After inhibitor treatments, cells were lysed with ice-cold cell lysis buffer and then protein concentration was determined using the Bio-Rad dye-binding assay. The changes in the phosphorylation or cleavage of the indicated molecules were determined with the PathScan Intracellular Signaling Array Kit (Chemiluminescent Readout), according to the manufacturer's procedure (Cell Signaling Technology), using 45 μg protein for each sample. Finally, the slide was incubated with Lumi-GLO/peroxide reagent for 2 min and exposed to Kodak BioMax X-ray films in dark room, **b** quantitation of mutant p53, ERK1/2, S6 Ribosomal Protein, PRAS40 and p38 MAPK phosphorylation. The quantitation was carried out by GelQuantNET program. The results are presented as fold changes/control. The experiment was performed twice with duplicate samples. The data are mean ± SEM (n = 4). Cntl, 0.5% DMSO-treated control group

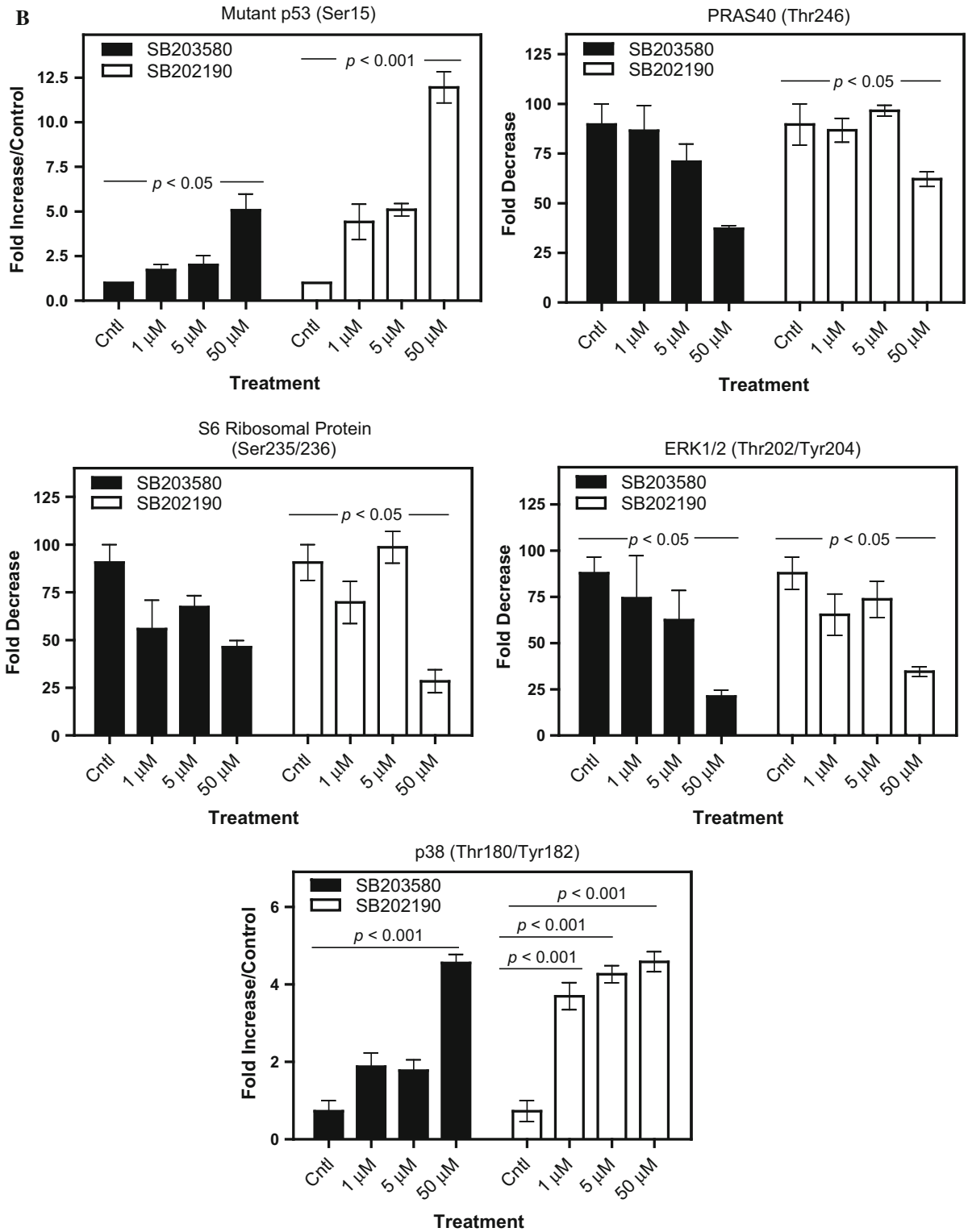

Fig. 5 continued

MAPK activity to successfully metastasize to distant sites (del Barco Barrantes and Nebreda 2012). However, the function of p38 MAPK in metastasis is controversial and not well-understood (Yan et al. 2013; Lopez-Bergami 2011). Both inhibitors did not show any cytotoxicity up to 10 μM concentrations; however, at 25, 50 or 100 μM concentrations, both inhibitors caused significant cytotoxicity as determined by MTT assay. It was determined that the IC_{50} value of SB203580 was 85.1 μM, while that of SB202190 was 46.6 μM, suggesting that SB202190 is slightly more effective than SB203580. Then we used the iCELLigence system to determine the effects of each inhibitor on cell proliferation in a dose- and time-dependent manner. This real-time assay showed that low doses of each inhibitor were not growth-inhibitory; however, 50 μM of each inhibitor showed significant growth-inhibition with SB202190 being more potent than SB203580. Afterwards, we examined the effect of 5 μM and 50 μM concentrations of each inhibitor on cell migration using wound assay. Both concentrations of each inhibitor caused a significant reduction in cell migration; however, SB202190 was again more significant than SB203580. Daroqui et al. (2012) similarly showed that SB202190 reduced cell migration of LM3 adenocarcinoma cell lines at a concentration of 10 μM. It was also reported that VEGF or MTA1 induced proliferation, migration and invasion of MDA-MB-231 cells can be prevented by 10 μM SB202190 for up to 24 h (Nagaraj et al. 2012). Du et al. (2013) showed that 30 μM or 10 μM of SB203580 did not cause significant growth-inhibition and apoptosis determined by flow cytometric analysis or cell migration as determined by a Transwell migration assay, respectively. Interestingly, they also showed that co-treatment of 10 μM SB203580 with 60 μM evodiamine increased the cell migration rate ~20%, compared to the 60 μM evodiamine alone (Du et al. 2013). In this study, we showed similarly that low doses of SB203580 did not cause significant growth-inhibition; however, on the contrary, both a low dose (5 μM) and a high dose (50 μM) of SB203580 caused significant cell migration-inhibition in MDA-MB-231 cell line using a wound assay.

We then studied the effect of each inhibitor on cell adhesion. As shown in the Result section, it was interestingly noticed that 1 μM concentration of SB203580 led to a significant increase in cell adhesion in E-plate L8 as compared to other doses (i.e., 5 and 50 μM). Likewise, Walsh et al. (2003) showed that inhibition of p38 by SB203580 (20 μM) increased SW620 cell adhesion in comparison to the DMSO vehicle control after 30 min of plating cells onto collagen I. Higher doses of SB203580 did not affect the adhesion of MDA-MB-231 cells seeded in E-plate L8. On the other hand, 50 μM SB202190 initially prevented cell adhesion for about 1.5 h, and then it was returned to the level of control cells after 2 h of treatment. It is believed that this is the first report indicating a reversible phenomenon of the prevention of cell adhesion following inhibition of p38 MAPK by SB202190 in MDA-MB-231 cells. This may be partly due to the transient inhibition of the secretion of cell matrix components by p38 MAPK inhibitor SB202190 at high concentrations.

To shed light on the mechanism of prevention of cell migration and growth by p38 MAPK inhibitors in MDA-MB-231 cell line, we examined the activation/inactivation of 18 signaling molecules by PathScan analysis. As presented in the current study, we determined downregulation of phosphorylation of ERK1/2, S6 Ribosomal Protein and PRAS40 in MDA-MB-231 cells in response to treatment with SB203580 and/or SB202190. Activation of both ERK1/2 and PRAS40 by phosphorylation generally exerts anti-apoptotic effects and promotes cell survival (Lu and Xu 2006; Lv et al. 2016). It is therefore believed that the growth inhibitory effects of p38 MAPK inhibitors SB203580 and SB202190 may be partly mediated through downregulation of ERK1/2 and PRAS40 phosphorylations. ERK1/2 pathway has been known to regulate NF-κB activation as well (Kim et al. 2014). Kim et al. (2014) have recently shown that Rg3, one of the major ingredients of heat-processed ginseng, induced apoptosis and inhibited cell proliferation in MDA-MB-231 cells, which is mediated by blocking NF-κB signaling via inactivation of phosphorylation of ERK as well as Akt. Similarly, Zhang et al. (2008) showed that butein, a polyphenolic compound, can inhibit migration and invasion through the ERK1/2 and NF-κB signaling pathways in human bladder cancer cells. Therefore, it is supposed that the growth and migration inhibitory effects of p38 MAPK inhibitors tested here may be mediated through the inactivation of ERK1/2 phosphorylation. One of the interesting results we observed here was increased Ser15 phosphorylation of mutant p53 (R280K) in MDA-MB-231 cells upon inhibition of p38 MAPK by

SB203580 and SB202190 inhibitors. Whether this increased Ser15 phosphorylation of mutant p53 has any role in the inhibition of growth and migration of MDA-MB-231 cell needs further investigation. The activation of wild-type p53 has been shown to inhibit NF-κB, which subsequently results in retardation of breast cancer cells migration by suppressing MMP-2 and MMP-9 (Adhikary et al. 2010). It is worth to further examine whether Ser15 phosphorylated mutant p53 similarly regulate NF-κB activation and secretion of matrix metalloproteases or not. Unexpectedly, it was found that both SB203580 and SB202190 treatments were associated with significant increases in p38 MAPK phosphorylation (at Thr180/Tyr182) in MDA-MB-231 cells after 24 h. This may be partly due to the fact that prolonged treatment (24 h) with relatively high concentrations of both inhibitors causes either inactivation of protein phosphatases acting on p38 MAPK or activation of an MLK-3-MKK4/MKK7-dependent signal transduction pathway. In fact, it was demonstrated that specific p38 MAPK inhibitors SB202190 or SB203580 induced the activation of the JNK pathway, depending on the MLK-3-MKK4/MKK7 signal transduction pathway (Muniyappa and Das 2008). The mixed-lineage kinases (MLKs) are a family of serine/threonine protein kinases that also have been found to activate p38 MAPK (Gallo and Johnson 2002). It would be interesting to examine whether the MLK-MKK4/MKK7 signal transduction pathway is activated in response to treatment with p38 MAPK inhibitors SB203580 and SB202190.

Acknowledgements This study was funded by Dumlupınar University Scientific Project No. 2015-85.

References

Adhikary A, Mohanty S, Lahiry L, Hossain DMS, Chakraborty S, Das T (2010) Theaflavins retard human breast cancer cell migration by inhibiting NF-κB via p53-ROS cross-talk. FEBS Lett 584:7–14

Aras B, Yerlikaya A (2016) Bortezomib and etoposide combinations exert synergistic effects on PC-3 prostate cancer line. Oncol Lett 11:3179–3184

Daroqui MC, Vazquez P, de Kier Bal, Joffé E, Bakın AV, Puricelli LI (2012) TGF-β autocrine pathway and MAPK signaling promote cell invasiveness and in vivo mammary adenocarcinoma tumor progression. Oncol Rep 28:567–575

del Barco Barrantes I, Nebreda AR (2012) Roles of p38 MAPKs in invasion and metastasis. Biochem Soc Trans 40:79–84

Du J, Wang X-F, Zhou Q-M, Zhang T-L, Lu Y-Y, Zhang H, Su S-B (2013) Evodiamine induces apoptosis and inhibits metastasis in MDA-MB-231 human breast cancer cells in vitro and in vivo. Oncol Rep 30:685–694

Edlund S, Bu S, Schuster N, Aspenström P, Heuchel R, Heldin NE, ten Dijke P, Heldin CH, Landström M (2003) Transforming growth factor-beta1 (TGF-beta)-induced apoptosis of prostate cancer cells involves Smad7-dependent activation of p38 by TGF-beta-activated kinase 1 and mitogen-activated protein kinase kinase 3. Mol Biol Cell 14:529–544

Freshney RI (2005) Culture of animal cells: a manual of basic techniques. Wiley, Hoboken

Gallo KA, Johnson GL (2002) Mixed-lineage kinase control of JNK and p38 MAPK pathways. Nat Rev Mol Cell Biol 3:663–672

Geiger PC, Wright DC, Han DH, Holloszy JO (2005) Activation of p38 MAP kinase enhances sensitivity of muscle glucose transport to insulin. Am J Physiol Endocrinol Metab 288:E782–E788

Gutiérrez-Uzquiza Á, Arechederra M, Bragado P, Aguirre-Ghiso JA, Porras A (2012) p38α mediates cell survival in response to oxidative stress via induction of antioxidant genes: effect on the p70S6K pathway. J Biol Chem 287:2632–2642

Huang S, New L, Pan Z, Han J, Nemerow GR (2000) Urokinase plasminogen activator/urokinase-specific surface receptor expression and matrix invasion by breast cancer cells requires constitutive p38alpha mitogen-activated protein kinase activity. J Biol Chem 275:12266–12272

Kim B-M, Kim D-H, Park J-H, Surh Y-J, Na H-K (2014) Ginsenoside Rg3 inhibits constitutive activation of NF-κB signaling in human breast cancer (MDA-MB-231) cells: ERK and Akt as potential upstream targets. J Cancer Prev 19:23–30

Koçak FE, Erdoğan E, Özyiğit F, Yerlikaya A (2013) Evaluation of antiproliferative and antimetastatic effects of heparin and erythropoietin on B16F10 melanoma cell line. Cell Mol Biol (Noisy-le-grand) 59:OL1894–OL1898

Kocanova S, Buytaert E, Matroule JY, Piette J, Golab J, de Witte P, Agostinis P (2007) Induction of heme-oxygenase 1 requires the p38MAPK and PI3K pathways and suppresses apoptotic cell death following hypericin-mediated photodynamic therapy. Apoptosis 12:731–741

Koul HK, Pal M, Koul S (2013) Role of p38 MAP kinase signal transduction in solid tumors. Genes Cancer 4:342–359

Kumar S, Jiang MS, Adams JL, Lee JC (1999) Pyridinylimidazole compound SB 203580 inhibits the activity but not the activation of p38 mitogen-activated protein kinase. Biochem Biophys Res Commun 263:825–831

Kumar B, Sinclair J, Khandrika L, Koul S, Wilson S, Koul HK (2009) Differential effects of MAPKs signaling on the growth of invasive bladder cancer cells. Int J Oncol 34:1557–1564

Lawson SK, Dobrikova EY, Shveygert M, Gromeier M (2013) p38alpha mitogen-activated protein kinase depletion and repression of signal transduction to translation machinery by miR-124 and -128 in neurons. Mol Cell Biol 33:127–135

Li W, Fan J, Chen M, Guan S, Sawcer D, Bokoch GM, Woodley DT (2004) Mechanism of human dermal fibroblast migration driven by type I collagen and platelet-derived growth factor-BB. Mol Biol Cell 15:294–3009

Liang CC, Park AY, Guan JL (2007) In vitro scratch assay: a convenient and inexpensive method for analysis of cell migration in vitro. Nat Protoc 2:329–333

Lopez-Bergami P (2011) The role of mitogen- and stress-activated protein kinase pathways in melanoma. Pigment Cell Melanoma Res 24:902–921

Lu Z, Xu S (2006) ERK1/2 MAP kinases in cell survival and apoptosis. IUBMB Life 58:621–631

Lv D, Liu J, Guo L, Wu D, Matsumoto K, Huang L (2016) PRAS40 deregulates apoptosis in Ewing sarcoma family tumors by enhancing the insulin receptor/Akt and mTOR signaling pathways. Am J Cancer Res 6:486–497

Miyake M, Goodison S, Urquidi V, Gomes Giacoia E, Rosser CJ (2013) Expression of CXCL1 in human endothelial cells induces angiogenesis through the CXCR2 receptor and the ERK1/2 and EGF pathways. Lab Invest 93:768–778

Muniyappa H, Das KC (2008) Activation of c-Jun N-terminal kinase (JNK) by widely used specific p38 MAPK inhibitor SB202190 and SB203580: a MLK-3-MKK7-dependent mechanism. Cell Signal 20:675–683

Nagaraj SRM, Balaraju Y, Shetty N, Salimath BP (2012) Metastatic events of MDA-MB-231 cells induced by angiogenic factors VEGF or MYA1 are inhibited by *Tinospora cordifolia* hexane fraction (tchf). IOSR J Pharm 2:24–30

Nemoto S, Xiang J, Huang S, Lin A (1998) Induction of apoptosis by SB202190 through inhibition of p38beta mitogen-activated protein kinase. J Biol Chem 273:16415–16420

Porras A, Guerrero C (2011) Role of p38α in apoptosis: implication in cancer development and therapy. Atlas Genet Cytogenet Oncol Haematol 15:316–326

Sicard P, Clark JE, Jacquet S, Mohammadi S, Arthur JS, O'Keefe SJ, Marber MS (2010) The activation of p38 alpha, and not p38 beta, mitogen-activated protein kinase is required for ischemic preconditioning. J Mol Cell Cardiol 48:1324–1328

Stone MK, Kolling GL, Lindner MH, Obrig TG (2008) p38 mitogen-activated protein kinase mediates lipopolysaccharide and tumor necrosis factor alpha induction of shiga toxin 2 sensitivity in human umbilical vein endothelial cells. Infect Immun 76:1115–1121

Valladares A, Alvarez AM, Ventura JJ, Roncero C, Benito M, Porras A (2000) p38 mitogen-activated protein kinase mediates tumor necrosis factor-alpha-induced apoptosis in rat fetal brown adipocytes. Endocrinology 141:4383–4395

Walsh MF, Thamilselvan V, Grotelueschen R, Farhana L, Basson MD (2003) Absence of adhesion triggers differential FAK and SAPKp38 signals in SW620 human colon cancer cells that may inhibit adhesiveness and lead to cell death. Cell Physiol Biochem 13:135–146

Xu L, Chen S, Bergan RC (2006) MAPKAPK2 and HSP27 are downstream effectors of p38 MAP kinase-mediated matrix metalloproteinase type 2 activation and cell invasion in human prostate cancer. Oncogene 25:2987–2998

Yan Q, Bach DQ, Gatla N, Sun P, Liu J-W, Lu J-Y, Paller AS, Wang X-Q (2013) Deacetylated GM3 promotes uPAR-associated membrane molecular complex to activate p38 MAPK in metastatic melanoma. Mol Cancer Res 11:665–675

Yerlikaya A, Dokudur H (2010) Investigation of the eIF2α phosphorylation mechanism in response to proteasome inhibition in melanoma and breast cancer cells. Mol Biol (Mosk) 44:760–768

Yerlikaya A, Erin N (2008) Differential sensitivity of breast cancer and melanoma cells to proteasome inhibitor velcade. Int J Mol Med 22:817–823

Yerlikaya A, Okur E, Ulukaya E (2012) The p53-independent induction of apoptosis in breast cancer cells in response to proteasome inhibitor bortezomib. Tumour Biol 33:1385–1392

Zhang L, Chen W, Li X (2008) A novel anticancer effect of butein: inhibition of invasion through the ERK1/2 and NF-κB signaling pathways in bladder cancer cells. FEBS Lett 582:1821–1828

Zhuang S, Demirs JT, Kochevar IE (2000) p38 mitogen-activated protein kinase mediates bid cleavage, mitochondrial dysfunction, and caspase-3 activation during apoptosis induced by singlet oxygen but not by hydrogen peroxide. J Biol Chem 275:25939–25948